IEEE Photonics Journal
An IEEE Photonics Society Publication

Phase-Sensitive Detection for Optical Sensing With Porous Silicon

Volume 4, Number 3, June 2012

J. Álvarez
N. Kumar
P. Bettotti
D. Hill, Member, IEEE
J. Martínez-Pastor

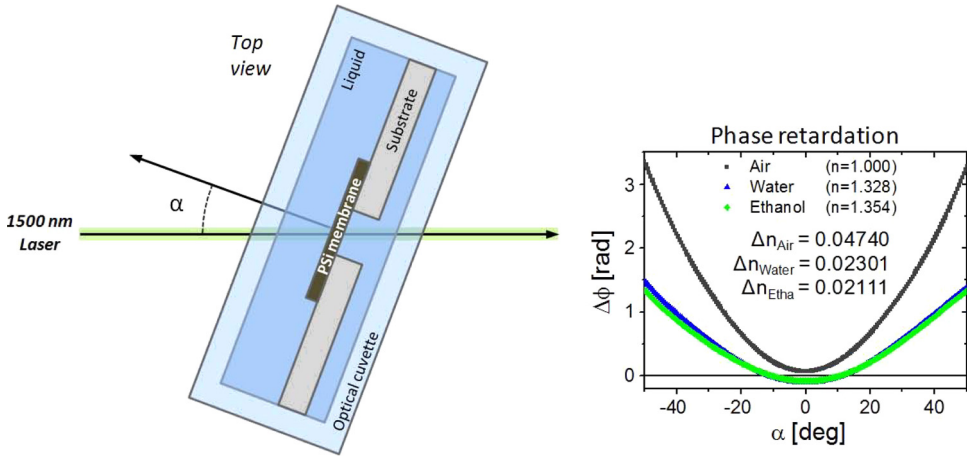

DOI: 10.1109/JPHOT.2012.2201461
1943-0655/$31.00 ©2012 IEEE

Phase-Sensitive Detection for Optical Sensing With Porous Silicon

J. Álvarez,[1] N. Kumar,[2] P. Bettotti,[2] D. Hill,[1] *Member, IEEE*, and J. Martínez-Pastor[1]

[1]UMDO, Materials Science Institute, University of Valencia, 46071 Valencia, Spain
[2]Nanoscience Laboratory, Department of Physics, University of Trento, 38050 Povo-Trento, Italy

DOI: 10.1109/JPHOT.2012.2201461
1943-0655/$31.00 ©2012 IEEE

Manuscript received March 10, 2012; revised May 18, 2012; accepted May 20, 2012. Date of publication May 25, 2012; date of current version June 13, 2012. This research was supported by the EC through the project FP7-257401 POSITIVE. Corresponding author: J. Álvarez (e-mail: jesus.alvarez@uv.es).

Abstract: We report on a photonic sensor with an ultralow limit of detection (LoD) based on a phase interrogation readout scheme together with an anisotropic porous silicon (PSi) membrane. First, the fabrication of porous free-standing membranes from medium doped (100) surface oriented silicon, with pore diameters suitable for the infiltration of biomolecules, around 50 nm, is reported. Then, the phase interrogation scheme for characterizing the PSi membranes is presented whose results show that while volumetric sensitivity increases with the membrane thickness, the resolution in the birefringence measurements decrease dramatically due to depolarization effects. The best LoD was found to be equal to 6.25×10^{-6} RIU, from the thinnest 10-μm-thick membrane. Finally, the thermooptic coefficient of the 10 μm membrane was measured in an aqueous environment and shown to be equal to 8×10^{-4} rad/°C.

Index Terms: Sensors, fabrication and characterization, subwavelength structures, scattering, metrology.

1. Introduction

Today there is an ever increasing need to develop sensitive optical and photonic biosensors capable of quantitative multiparameter measurements for medical analyzes, food quality control, drug development, environmental monitoring and research applications [1], [2]. Many are capable of being incorporated into lab-on-a-chip devices for the added advantages of performing measurements at the point-of-care and at an affordable cost [3]. A key component of these biosensors is the transducer, which is responsible for the transformation of variations in physical environmental parameters (e.g., refractive index) into a measurable signal (e.g., optical power). Porous silicon (PSi) as a transducer has unique properties. Its huge internal surface/volume ratio (on the order of 100 m^2/cm^3) when functionalized by a suitable surface chemistry [4] permits a greater number of target molecules to be captured per chip area compared to planar sensors, allowing a higher integration of assays [5]. In doing so, the surface can be left either hydrophobic or hydrophilic to allow a large range of biomolecules to immobilize within the pores. Furthermore, its porosity, thickness and pore diameters can be tuned according to the biorecognition application by changing the etching conditions during the fabrication process [4].

To date, a large volume of work has been done in the pursuit of realizing optical sensors based on PSi [6], [7]. The simplest such device consists of a PSi layer etched into p-type silicon. The presence of a different substance in the PSi layer modifies its effective refractive index, producing a

shift in the fringe spectrum [8]. More complex designs such as multilayer structures have also been studied for biosensing purposes [9]. In this case, a defect layer is buried in a multilayer structure composed of successive layers of high and low refractive index PSi. A narrow resonance is observed in the transmission spectra whose position is highly sensitive to the presence of molecules inside the defect region [10], [11]. The main limitation of these approaches lies in the difficulty for the target molecules to infiltrate the cavity region due to differences between the porosity or pore sizes of the multilayer structure. Photonic waveguides made from PSi have been also proposed as sensors [12] where light is confined and propagated in a medium porosity layer on top of a high porosity layer. The sensing mechanism is based on the variation of waveguide-mode excitation angle when the analyte enters into the waveguide. More recently, another design based on the Bloch surface waves present at the truncated end of a 1-D photonic has been presented for sensing applications [13]. Finally, other designs have been proposed that utilize the anisotropy of PSi and the sensitivity of the associated birefringence to refractive index changes within the pores. The first uses PSi made from (110) surface oriented silicon as this presents high birefringence [14], [15], others are based on PSi prepared from (100) surface oriented silicon as this too presents high anisotropy when the incident light direction is tilted with respect to pore grown direction due to the difference in the effective index between the ordinary, no, and extraordinary, ne, directions. To date this dependence has only been exploited for vapor sensing through nanoporous silicon membranes [16], [17].

In our previous work [18] we studied the sensing properties of PSi membranes in the wavelength range from 600 nm to 1600 nm. The long term stability of the fabricated membranes was demonstrated when the PSi was thermally oxidized. Furthermore, a new model was developed in order to determine the depolarization sources and its contribution to the overall depolarization process.

In the present paper, we report on an ultralow limit of detection (LoD) sensing mechanism based on a phase interrogation scheme for characterizing the optical anisotropy of mesoporous silicon membranes. First, we report how PSi membranes with thickness of 10, 30 and 60 μm were fabricated from n-type (100) surface oriented silicon allowing a pore size desirable for biomolecules infiltration, around 50 nm. The readout scheme for the birefringence measurements is then presented. It is based on the use of a photoelastic modulator to modulate the light polarization, which allows a resolution to be reached of down to 10^{-7} rad. We then show how with this scheme the birefringence of the fabricated membranes was obtained by means of measuring the phase retardation as a function of the light incidence angle. Thereafter sensing results from immersing the samples in several solutions of water and ethanol are reported, demonstrating that thicker membranes are more sensitive. The resolutions that can be reached with the different membranes when measured are then shown where it can be clearly seen that when the sample thickness increases the depolarization does also, which deteriorates the resolution in the phase retardation measurement. Combining the sensitivity and the resolution results, we show that the thinnest membrane (10 μm) presents the lowest LoD, being equal to 6.25×10^{-6} RIU (Refractive Index Unit). The last section of this work shows the characterization of the thermal stability of the 10 μm thin membrane in aqueous environment, showing a thermooptic coefficient of 8×10^{-4} rad/RIU.

2. Fabrication

PSi is typically prepared by electrochemical etching of silicon using HF dissolved in water or ethanol. Parameters such as pore size, porosity and layer thickness can be adjusted by correctly choosing the resistivity of the silicon wafer, the HF concentration and the etch time [19]. In the present work, the fabrication of the macroporous silicon membranes was carried out using an n-type (100) surface oriented silicon wafer with a resistivity of 0.01 $\Omega \cdot$cm. Membranes with thicknesses of 10, 30 and 60 μm were obtained via the following two step process; the first consisted of etching the PSi layer on the silicon wafer using HF with a concentration of 17% diluted in a solution of water and ethanol; the second consisted of applying a large current in order to completely dissolve the underneath of the etched layer [20]. The current density used for producing

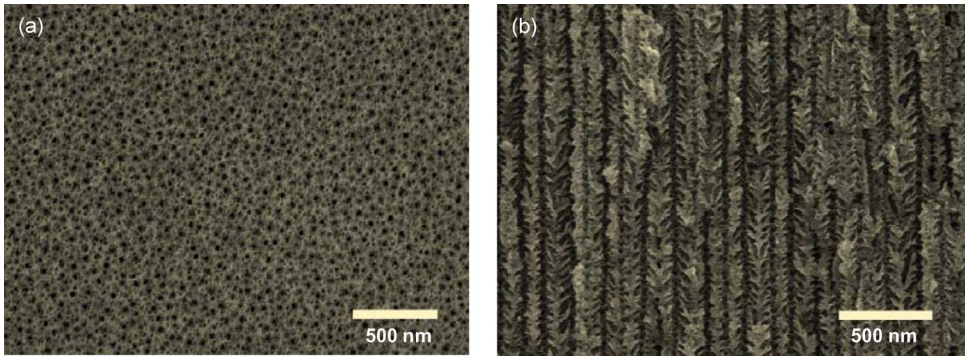

Fig. 1. (a) Surface SEM image of one of the fabricated samples made from (100) surface oriented silicon. (b) Cross section SEM image of the same sample. Pores diameter is around 50 nm.

the membranes was 25 mA/cm^2, and by applying it during 360, 600 and 1200 seconds, the 10, 30 and 60 μm thick membranes were produced respectively with etch rates of 28 nm/s for the 10 μm thick sample and 50 nm/s for the 30 and 60 μm thick samples. Scanning electron microscope (SEM) images of the fabricated samples (Fig. 1) show that the pore sizes of the samples were around 50 nm. An effective refractive index of 2.9 for the samples was measured from the fringes of the reflectance spectra in the infrared region, which corresponds to a porosity of about 0.3. After the optical characterization of several membranes with the same thickness we found that the differences in their optical properties (absorbance and birefringence) was smaller than 5%, which demonstrates the reliability of the fabrication process.

After the two step fabrication process, the free-standing membranes were mounted on borosilicate glass frames using a 1 μm thick of PMMA (Poly(methyl methacrylate)) resist as the adhesion layer between the borosilicate frame and the free-standing PSi membrane. Before the optical characterization, the PSi samples were thermally oxidized at 200 °C for 12 hours. This oxidation process has two purposes; first a thin silicon dioxide layer is formed on the pore walls so as to stabilize them, reducing the drift in effective refractive index by about one order of magnitude respect to the unoxidized samples [18]. Secondly, the thin silicon dioxide layer increases the hydrophilicity of the samples [4] for the liquids in the subsequent sensing experiments.

3. Theory

The optical anisotropy of PSi is a well known property for PSi fabricated (100) surface oriented silicon [17]. In order to simulate the birefringence of mesoporous silicon we used the generalized Bruggeman model [21] which assumes the static field condition, which is satisfied when the wavelength of light is much longer than the transverse pore size. In our case the static field condition is satisfied since pore diameters are in the order of 50 nm and working wavelength is 1500 nm. The generalized Bruggeman model is described by

$$\sum_i f_i \frac{n_i^2(\lambda) - n_{e,o}^2(\lambda)}{n_{e,o}^2(\lambda) + L_{e,o} \cdot \left(n_i^2(\lambda) - n_{e,o}^2(\lambda)\right)} = 0 \tag{1}$$

where f_i is the volume fraction of the different materials that form the PSi membrane, $n_i(\lambda)$ their refractive indices, and $L_{e,o}$ are the depolarization tensor factors. The unknown $n_e(\lambda)$ and $n_o(\lambda)$ are the extraordinary and ordinary refractive and are related to the birefringence by means of $\Delta n(\lambda) = n_e(\lambda) - n_o(\lambda)$. Due to in the present work all the results are obtained for a wavelength of 1500 nm, from now on we will consider the values of $n_{i,e,o}$, as $n_{i,e,o}(\lambda = 1500nm)$. The depolarization tensor factors L_e and L_o describe the screening efficiency of external electromagnetic field inside the pores. For pores grown perpendicular to the surface they have values of $L_e = 0$ and $L_o = 0.5$ [22]. The generalized Bruggeman model has been used in the literature to

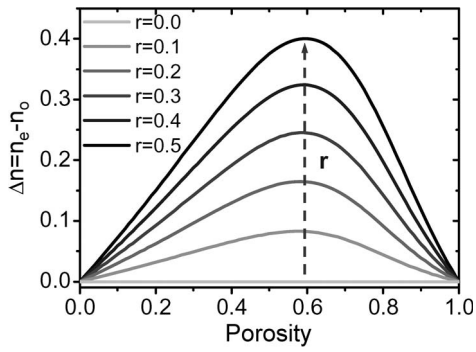

Fig. 2. Simulated birefringence as a function of the porosity for different values of r (r represents the amount of pores in the $\langle 100 \rangle$ direction over the total pores volume).

simulate the birefringence of porous alumina membranes with pore sizes around 50 nm giving good accordance between the measured results and the simulated ones [22]. On the contrary, preliminary results on (100) PSi showed a discrepancy of one order of magnitude between the measured birefringence values and the simulated ones using the Bruggeman model [23]. The main reason of this discrepancy is because in mesoporous silicon fabricated from n-type substrates the pores not only grow in the $\langle 100 \rangle$ direction but also in the $\langle 113 \rangle$ directions [24]. These branches can be clearly seen in Fig. 1(b) and so for a more realistic simulated birefringence values, the pores grown in the $\langle 113 \rangle$ direction must be taken into account. For that we propose a simple method based on modifying the depolarization tensor factors by

$$L_{e,o} = r \cdot L_{e,o_{\langle 100 \rangle}} + (1 - r) \cdot L_{e,o_{\langle 113 \rangle}} \tag{2}$$

where r is a parameter that relates the pore volume in the $\langle 100 \rangle$ direction to that of the total pore volume. According to the data given in the literature [22], the depolarization tensors factors are $L_{e_{\langle 100 \rangle}} = 0.0$ and $L_{o_{\langle 100 \rangle}} = 0.5$ when the pores are modeled as cylinders that grow perpendicular to the sample surface. In accounting for the anisotropy of the pores grown in the $\langle 113 \rangle$ direction, due to the symmetry with respect to the $\langle 100 \rangle$ direction, the depolarization tensor factors were assumed to be $L_{e,o_{\langle 113 \rangle}} = 1/3$. Using the generalized Bruggeman model and the new depolarization tensor factors (1) was solved as a function of the porosity for different values of the r coefficient (Fig. 2).

Birefringence values are related to the phase retardation of the light parallel and perpendicular components by the following equation [17]:

$$\Delta\phi(\alpha) = \frac{2\pi}{\lambda}(d_e(\alpha) \cdot \eta_e(\alpha) - d_o(\alpha) \cdot \eta_o(\alpha)) \tag{3}$$

where λ is the wavelength the light source, d_e, d_o, η_e, η_o are given by the following expressions:

$$d_{e,o}(\alpha) = \frac{d}{\sqrt{1 - \frac{\sin^2\alpha}{n^2_{e,o}(\alpha)}}} \tag{4}$$

$$\eta_e(\alpha) = \frac{1}{\sqrt{\frac{\sin^2\alpha}{n^2_e(\alpha)} + \frac{\cos^2\alpha}{n^2_o(\alpha)}}} \tag{5}$$

$$\eta_o(\alpha) = n_o \tag{6}$$

being d the PSi membrane thickness, α the angle between the light beam and the vector normal to the PSi surface, and n_e, n_o the ordinary and extraordinary refractive index.

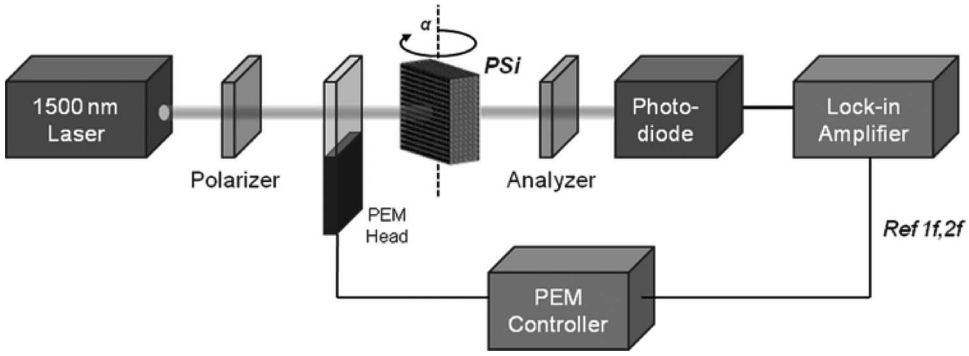

Fig. 3. Setup used for the phase retardation measurement of the fabricated PSi membranes.

4. Experimental

Optical birefringence can be measured by a wide variety of methods; the simplest one is based on the measurement of the transmitted light through a sample when it is placed between crossed polarizers [17]. Although this method is simple to implement, it does not provide highly accurate results and instead a photoelastic modulator (PEM) can be used [25]. In recent years, the use of a PEM has also been proposed to help improve upon the LoD of optical sensors based on surface plasmon resonance (SPR) [26] and plasmonic gratings [27].

For the measurement of phase retardation associated with the birefringence of the PSi samples, the optical setup used is the one depicted in Fig. 3. Specifically, the output light from a stabilized 1500 nm laser (New Focus TLB-6326) is collimated and the light linearly polarized. The continuous light was phase modulated by the PEM through sinusoidal variation of its polarization. The modulated light passes through the PSi sample, which was mounted on a motorized rotation stage (Thorlabs CR1-7Z) which permits changing the sample rotation angle. After passing the PSi sample and a second polarizer the light is detected by an InGaAs photodiode which is connected to a lock-in amplifier (SR-810) in order to perform the synchronous detection and measure the first and second harmonic amplitude of the signal.

The phase retardation is related to the first and second harmonics of the modulated light by [28]

$$\Delta\phi(\alpha) = \arctan\left(\frac{V_{1f}(\alpha)}{V_{2f}(\alpha)} \cdot \frac{J_2(A_0)}{J_1(A_0)}\right) \tag{7}$$

where α is the angle between the light beam and the vector normal to the PSi surface, V_{1f}, V_{2f} are the amplitude of the first and second harmonic and $J_1(A_0)$, $J_2(A_0)$ the first Bessel function of first and second order, being A_0 the amplitude of the modulating signal (in radians).

Before beginning with sample characterization the resolution of the setup was tested by taking multiple measurements of a quartz sample with a known birefringence. The measured values had a Gaussian distribution with a standard deviation equal to 10^{-7} rad. By adopting the convention that the resolution is given by the standard deviation when the values have a Gaussian distribution, we obtain the resolution of our measurement system as 10^{-7} rad.

5. Results and Discussion

Using the optical setup described in Section IV the phase retardation of the fabricated samples was measured as a function of the sample rotation angle. The first measurements were carried out in order to determine the birefringence of the different samples. After that, the phase retardation was measured when different solutions of water and ethanol filled the membranes pores. For this purpose the samples were immersed in a optical cuvette (mounted over the rotation stage) were the different solutions of water and were introduced. The LoD of the system was also obtained and lastly, the effect that temperature variation has over the PSi transducer performance was determined.

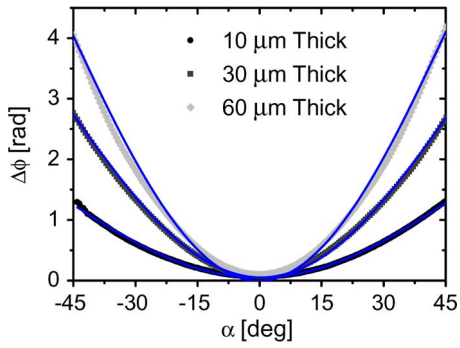

Fig. 4. Phase retardation as a function of the sample rotation angle for samples with thicknesses of 10, 30 and 60 μm. Blue lines represent the theoretical values obtained from the fitting of (7) to experimental ones.

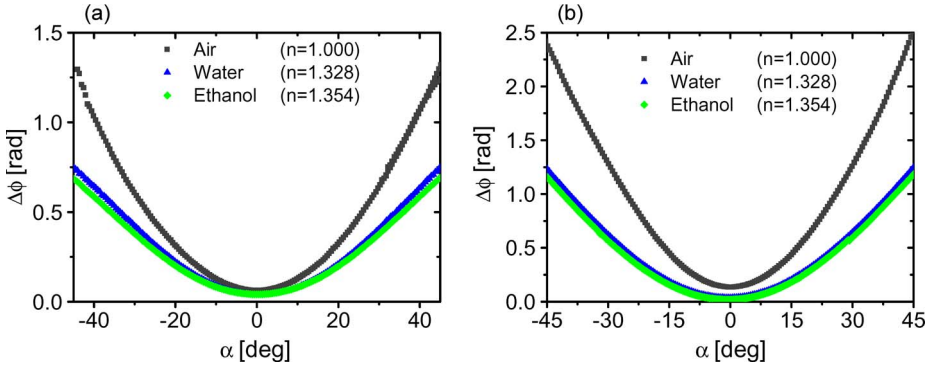

Fig. 5. Phase retardation as a function of the light incidence angle for pores filled with air (gray line), water (blue line) and ethanol (green line) for a 10 μm thick sample (a), and 30 μm thick sample (b).

5.1. Birefringence

The birefringence of the fabricated mesoporous membranes is clearly related to the sensitivity, with membranes being more sensitive when they have greater birefringence. The birefringence of the membranes was obtained by fitting the measured phase retardation values to the theoretical values given by (3). The measured phase retardation values of the fabricated samples are shown in Fig. 4 where blue lines represent the theoretical values obtained from the fitting. Birefringence values of 0.06607, 0.04401 and 0.03712 were obtained for the 10, 30 and 60 μm samples, respectively. A clear decrease in birefringence values when sample thicknesses increase is seen. A SEM inspection of sample cross sections confirmed that this was due to more pores growing in the $\langle 113 \rangle$ directions when the etching time increases.

5.2. Sensitivity

One of the two key figures of merit for an optical transducer is the sensitivity of the optical response to given changes in the refractive index of its environment. In this section the sensitivities of the three membranes are obtained by measuring the samples phase retardations when immersed in liquids with different refractive indices. The liquids employed were water ($n_{Water} = 1.328$) and ethanol ($n_{Ethanol} = 1.354$), as well as solutions of ethanol in water with concentrations of 50:50 and 75:25.

The measurements were carried out by the process explained in the previous section with the only difference being that the samples were immersed in the liquids. Results in air, water and ethanol for the 10 and 30 μm thick samples are shown in Fig. 5. Three clear annotations can be

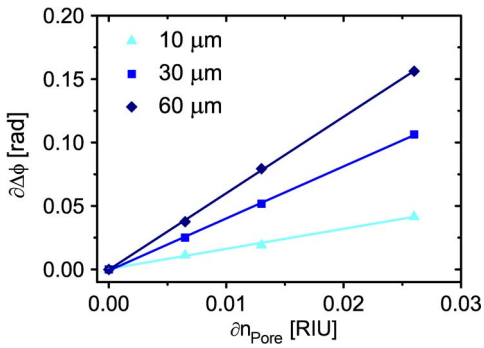

Fig. 6. Phase retardation shifts for samples rotation angle of 45° as a function of the refractive index of the material that fills the pores for samples with thickness 10, 30 and 60 μm (dots). A solid line represents the linear fitting of the experimental data, showing sensitivities of 1.6 rad/RIU, 4 and 6 rad/RIU for the 10, 30 and 60 m thick, respectively.

made: firstly, a reduction in the phase retardation is observed when the refractive index of the liquids that fill the samples increases. Secondly, both phase retardation and its derivative are higher for thicker samples, thus greater sensitivities are also expected. Thirdly, the change in the phase retardation and therefore sensitivity increases with the incidence angle.

Fixing the sample azimuthal rotation angle to 45° the phase retardation was measured when the samples were immersed in a solution of water:ethanol $= 100:0, 25:75, 50:500:100$. Fig. 6 shows the phase retardation change as a function of the solution refractive index showing a linear behavior between the liquids refractive index and the change in the phase retardation value. The phase retardation change was fitted to a linear function showing sensitivities of 1.6, 4 and 6 rad/RIU.

5.3. Limit of Detection

While the sensitivity gives an idea of the optical transducer performance, the usually more important figure of merit is the smallest refractive index change that it can respond to and be resolved, i.e., measure accurately, that is the LoD. The limit of the detection relates the sensitivity of the transducer to the resolution of the readout system by

$$LoD[RIU] = \frac{\sigma[rad]}{\partial\Delta\phi[rad/RIU]} \tag{8}$$

where σ is the measurement system resolution and $\partial\Delta\phi$ is the transducer sensitivity.

As previously reported [18], [29], light scattering in an inhomogeneous medium like PSi generates incoherent light which depolarizes the light thereby deteriorating the system resolution which for our system was measured at 10^{-7} rad for a quartz reference sample. The amount of depolarized light increases with the PSi sample thickness, so the system resolution needs to be tested for PSi samples with different thickness. The resolution of the measurement system was therefore obtained from the standard deviation of the birefringence measured values of the fabricated PSi samples (10, 30 and 60 μm thick) when they were immersed in water. We observed that the resolution decreases dramatically when the thickness of the samples increases: going from 1×10^{-5} to 5×10^{-5} to 5×10^{-4} for 10, 30 and 60 μm, respectively.

Combining the values of the sensitivity obtained in the previous section and the resolution values obtained above, the limits of detection that can be reached with each membrane can be determined from (8). Table 1 shows the sensitivity, resolution and LoD values for all the membranes measured. We can see that although the sensitivity increases with the sample thickness, at the same time the resolution decreases dramatically due to the depolarization. The thinnest fabricated membrane (10 μm) is therefore potentially the most suitable for biosensing purposes due to its smaller LoD.

TABLE 1

Sensitivity, resolution and LoD of the three types of PSi samples measured in aqueous environment.

Thickness $[\mu m]$	Sensitivity $[rad/RIU]$	Resolution $[rad]$	LoD $[RIU]$
10	1.6	$1x10^{-5}$	$6.25x10^{-6}$
30	4.5	$5x10^{-5}$	$1.25x10^{-5}$
60	6	$1x10^{-4}$	$8.33x10^{-5}$

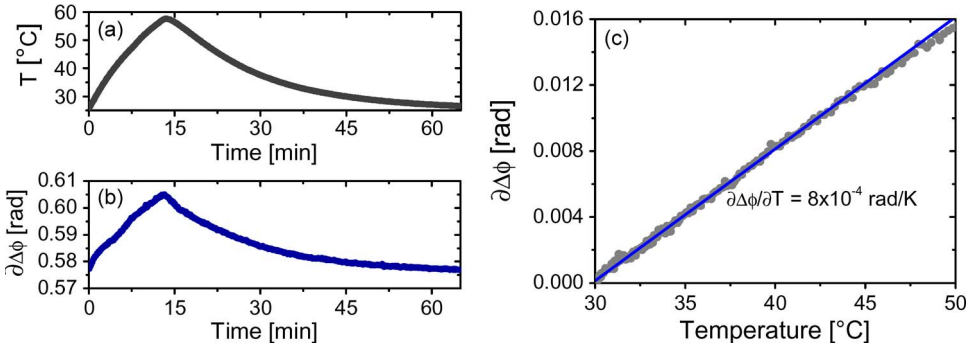

Fig. 7. (a) Sample temperature variation as a function of time. (b) Phase retardation as a function of time. (c) Phase retardation change as a function of the sample temperature.

5.4. Thermal Stability

The refractive index of the materials used to develop photonic or optical sensors, such as semiconductors or glasses is temperature dependent. Due to that, the optical properties of the transducer not only change when the refractive index of the surrounding media does, but it also changes as the temperature of the same media does.

In order to quantify this change for biosensing the thermal stability of a PSi membrane in the same aqueous environment was determined. To do so, the sample holder was placed in a closed chamber where the temperature could be increased from ambient to 50 °C and a platinum temperature sensor placed within it in order to monitor its temperature. As the chamber was heated both the phase retardation as well as the sample temperature were monitored in time during a rising and falling cycle [Fig. 7(a) and (b)]. The phase retardations was plotted against the chamber temperature [Fig. 7(c)] showing a liner dependence with a slope of 8×10^{-4} rad/°C. This value could be used to determine the resolution needed for the thermal stabilization system within an instrument based on such a sensing mechanism. Thus for a resolution in the phase retardation measurement of 10^{-5} rad, a thermal control with a temperature change of 12.5 mK will produce a change in the phase retardation equal to the system resolution. This means that an active thermal control with a setpoint temperature resolution of 1 mK will provide a thermal stability for phase variation one order of magnitude better than that of the overall system phase resolution.

6. Conclusion

A highly sensitive device for biosensing purposes has been presented that is based on the use of a phase retardation readout scheme for the characterization of optical anisotropic of mesoporous silicon membranes. The fabrication of mesoporous free-standing membranes with pore diameters around 50 nm and thickness of 10, 30 and 60 μm were reported, which are suitable for biosensing.

The results of the anisotropy characterization of the fabricated membranes showed that the birefringence decreases with the sample thickness due to the amount of pores that grow in the ⟨113⟩ directions having increased with the etch time. The sensing experiments carried out with the membranes using different solutions of water and ethanol showed that the thinner membranes (10 μm thick) present the lowest LoD, equal to 6.25×10^{-6} RIU. The thicker membranes have a worse LoD due to the increase in depolarization worsening the resolution of the measurement system. In the last section of the work the thermooptic coefficient of a 10 μm thick membrane is measured in aqueous environment at 8×10^{-4} rad/°C.

Acknowledgment

The authors acknowledge Julian Heredero Calero for his design and mechanization of the sample holder and temperature chamber.

References

[1] X. Fan, I. M. White, S. I. Shopova, H. Zhu, J. D. Suter, and Y. Sun, "Sensitive optical biosensors for unlabeled targets: A review," *Anal. Chim. Acta*, vol. 620, no. 1/2, pp. 8–26, Jul. 2008. [Online]. Available: http://www.sciencedirect.com/science/article/pii/S0003267008009343

[2] D. Hill, "Advances in nanophotonic sensing technologies during three international label-free lab-on-chip projects," *BioNanoScience*, vol. 1, pp. 162–172, 2011, DOI:10.1007/s12668-011-0026-1. [Online]. Available: http://dx.doi.org/10.1007/s12668-011-0026-1

[3] F. S. Ligler, "Perspective on optical biosensors and integrated sensor systems," *Anal. Chem.*, vol. 81, no. 2, pp. 519–526, Jan. 2009. [Online]. Available: http://pubs.acs.org/doi/abs/10.1021/ac8016289

[4] K. A. Kilian, T. Bocking, and J. J. Gooding, "The importance of surface chemistry in mesoporous materials: Lessons from porous silicon biosensors," *Chem. Commun.*, vol. 6, pp. 630–640, 2009. [Online]. Available: http://dx.doi.org/10.1039/B815449J

[5] C. Li, R. Orobtchouk, T. Benyattou, A. Belarouci, Y. Chevolot, V. Monnier, E. Souteyrand, E. Gerelli, and C. Jamois, *New concepts of integrated photonic biosensors based on porous silicon, Biosensors—Emerging Materials and Applications*, P. A. Serra, Ed. Rijeka, Croatia: InTech., 2011. [Online]. Available: http://www.intechopen.com/articles/show/title/new-concepts-of-integrate d-photonic-biosensors-based-on-porous-silicon

[6] A. Jane, R. Dronov, A. Hodges, and N. H. Voelcker, "Porous silicon biosensors on the advance," *Trends Biotechnol.*, vol. 27, no. 4, pp. 230–239, Apr. 2009. [Online]. Available: http://www.sciencedirect.com/science/article/B6TCW-4VR0MBX-2/2/c9730bc89c2ee8572fb4decbb1a64ce2

[7] G. Korotcenkov and B. K. Cho, "Porous semiconductors: Advanced material for gas sensor applications," *Crit. Rev. Solid State Mater. Sci.*, vol. 35, no. 1, pp. 1–37, 2010. [Online]. Available: http://www.tandfonline.com/doi/abs/10.1080/10408430903245369

[8] V. S.-Y. Lin, K. Motesharei, K.-P. S. Dancil, M. J. Sailor, and M. R. Ghadiri, "A porous silicon-based optical interferometric biosensor," *Science*, vol. 278, no. 5339, pp. 840–843, Oct. 1997. [Online]. Available: http://www.sciencemag.org/content/278/5339/840.abstract

[9] V. Mulloni and L. Pavesi, "Porous silicon microcavities as optical chemical sensors," *Appl. Phys. Lett.*, vol. 76, no. 18, pp. 2523–2525, May 2000. [Online]. Available: http://link.aip.org/link/?APL/76/2523/1

[10] H. Ouyang, M. Christophersen, R. Viard, B. Miller, and P. Fauchet, "Macroporous silicon microcavities for macromolecule detection," *Adv. Funct. Mater.*, vol. 15, no. 11, pp. 1851–1859, Nov. 2005. [Online]. Available: http://dx.doi.org/10.1002/adfm.200500218

[11] L. M. Bonanno and L. A. DeLouise, "Whole blood optical biosensor," *Biosens. Bioelectron.*, vol. 23, no. 3, pp. 444–448, Oct. 2007. [Online]. Available: http://www.sciencedirect.com/science/article/pii/S0956566307002795

[12] G. Rong, A. Najmaie, J. Sipe, and S. Weiss, "Porous silicon waveguides for DNA detection," in *Proc. 3rd IEEE Int. Conf. Group IV Photon.*, 2006, pp. 13–15.

[13] F. Michelotti, B. Sciacca, L. Dominici, M. Quaglio, E. Descrovi, F. Giorgis, and F. Geobaldo, "Fast optical vapour sensing by Bloch surface waves on porous silicon membranes," *Phys. Chem. Chem. Phys.*, vol. 12, no. 2, pp. 502–506, 2010. [Online]. Available: http://dx.doi.org/10.1039/B914280K

[14] M. Kompan, J. Salonen, and I. Shabanov, "Anomalous birefringence of light in free-standing samples of porous silicon," *J. Exp. Theor. Phys.*, vol. 90, no. 2, pp. 324–329, Feb. 2000, DOI:10.1134/1.559107. [Online]. Available: http://dx.doi.org/10.1134/1.559107

[15] E. Gross, D. Kovalev, N. Künzner, V. Y. Timoshenko, J. Diener, and F. Koch, "Highly sensitive recognition element based on birefringent porous silicon layers," *J. Appl. Phys.*, vol. 90, no. 7, pp. 3529–3532, Oct. 2001. [Online]. Available: http://link.aip.org/link/?JAP/90/3529/1

[16] R. Liu, T. A. Schmedake, Y. Y. Li, M. J. Sailor, and Y. Fainman, "Novel porous silicon vapor sensor based on polarization interferometry," *Sens. Actuators B, Chem.*, vol. 87, no. 1, pp. 58–62, Nov. 2002. [Online]. Available: http://www.sciencedirect.com/science/article/B6THH-46RVCRW-3/2/f3d84c4895e7cee786c4b3a91cf3bc3d

[17] O B.-H., R. Liu, Y. Y. Li, M. Sailor, and Y. Fainman, "Vapor sensor realized in an ultracompact polarization interferometer built of a freestanding porous-silicon form birefringent film," *IEEE Photon. Technol. Lett.*, vol. 15, no. 6, pp. 834–836, Jun. 2003.

[18] J. Álvarez, P. Bettotti, I. Suárez, N. Kumar, D. Hill, V. Chirvony, L. Pavesi, and J. Martínez-Pastor, "Birefringent porous silicon membranes for optical sensing," *Opt. Exp.*, vol. 19, no. 27, pp. 26 106–26 116, Dec. 2011. [Online]. Available: http://www.opticsexpress.org/abstract.cfm?URI=oe-19-27-26106
[19] Z. Gaburro, P. Bettotti, M. Saiani, L. Pavesi, L. Pancheri, C. J. Oton, and N. Capuj, "Role of microstructure in porous silicon gas sensors forNO_2," *Appl. Phys. Lett.*, vol. 85, no. 4, pp. 555–557, Jul. 2004. [Online]. Available: http://link.aip.org/link/?APL/85/555/1
[20] C. J. Oton, M. Ghulinyan, Z. Gaburro, P. Bettotti, L. Pavesi, L. Pancheri, S. Gialanella, and N. E. Capuj, "Scattering rings as a tool for birefringence measurements in porous silicon," *J. Appl. Phys.*, vol. 94, no. 10, pp. 6334–6340, Nov. 2003. [Online]. Available: http://link.aip.org/link/?JAP/94/6334/1
[21] J. E. Spanier and I. P. Herman, "Use of hybrid phenomenological and statistical effective-medium theories of dielectric functions to model the infrared reflectance of porous sic films," *Phys. Rev. B*, vol. 61, no. 15, pp. 10 437–10 450, Apr. 2000. [Online]. Available: http://link.aps.org/doi/10.1103/PhysRevB.61.10437
[22] A. Lutich, M. Danailov, S. Volchek, V. Yakovtseva, V. Sokol, and S. Gaponenko, "Birefringence of nanoporous alumina: Dependence on structure parameters," *Appl. Phys. B, Lasers Opt.*, vol. 84, pp. 327–331, 2006. [Online]. Available: http://dx.doi.org/10.1007/s00340-006-2262-6
[23] J. Alvarez, P. Bettotti, N. Kumar, I. Suarez, D. Hill, and J. Martinez-Pastor, "Highly-sensitive anisotropic porous silicon based optical sensors," in *Proc. SPIE—Frontiers Biol. Detect., Nanosens. Syst. IV*, 2012, vol. 8212, no. 1, p. 821 209. [Online]. Available: http://link.aip.org/link/?PSI/8212/821209/1
[24] S. Rönnebeck, S. Ottow, J. Carstensen, and H. Föll, "Crystal orientation dependence of macropore formation in n-Si with backside-illumination in HF-electrolyte," *J. Porous Mater.*, vol. 7, no. 1–3, pp. 353–356, Jan. 2000, DOI:10.1023/A:1009639105357. [Online]. Available: http://dx.doi.org/10.1023/A:1009639105357
[25] C. F. Wong, "Birefringence measurement using a photoelastic modulator," *Appl. Opt.*, vol. 18, no. 23, pp. 3996–3999, Dec. 1979. [Online]. Available: http://ao.osa.org/abstract.cfm?URI=ao-18-23-3996
[26] D. J. Diner, A. Davis, B. Hancock, G. Gutt, R. A. Chipman, and B. Cairns, "Dual-photoelastic-modulator-based polarimetric imaging concept for aerosol remote sensing," *Appl. Opt.*, vol. 46, no. 35, pp. 8428–8445, Dec. 2007. [Online]. Available: http://ao.osa.org/abstract.cfm?URI=ao-46-35-8428
[27] M. Maisonneuve, O. d'Allivy Kelly, A.-P. Blanchard-Dionne, S. Patskovsky, and M. Meunier, "Phase sensitive sensor on plasmonic nanograting structures," *Opt. Exp.*, vol. 19, no. 27, pp. 26 318–26 324, Dec. 2011. [Online]. Available: http://www.opticsexpress.org/abstract.cfm?URI=oe-19-27-26318
[28] F. Benabid, M. Notcutt, L. Ju, and D. Blair, "Birefringence measurements of sapphire test masses for laser interferometer gravitational wave detector," *Phys. Lett. A*, vol. 237, no. 6, pp. 337–342, Jan. 1998. [Online]. Available: http://www.sciencedirect.com/science/article/pii/S0375960197008189
[29] K. H. Jun and K. S. Lim, "Simulation of the depolarization effect in porous silicon," *Appl. Opt.*, vol. 42, no. 7, pp. 1211–1215, Mar. 2003. [Online]. Available: http://ao.osa.org/abstract.cfm?URI=ao-42-7-1211